ACS OMEGA

Open Access

http://pubs.acs.org/journal/acsodf

Article

Effect of PTFGRN Expression on the Proteomic Profile of A431 Cells and Determination of the PTGFRN Interactome

Jorge Marquez, Mehari M. Weldemariam, Jianping Dong, Jun Hayashi, Maureen A. Kane, and Ginette Serrero*

Cite This: *ACS Omega* 2024, 9, 14381−14387

Read Online

ACCESS | Metrics & More | Article Recommendations | Supporting Information

ABSTRACT: Prostaglandin F2 receptor negative regulator (PTGFRN) is a transmembrane protein whose expression has been previously implicated in cancer metastasis. However, the exact molecular mechanisms by which PTGFRN influences cancer progression are still unknown. As such, our laboratory set out to investigate how PTGFRN knockdown affected the expression of other proteins. We also carried out coimmunoprecipitation experiments using a monoclonal anti-PTGFRN antibody. We employed mass spectrometry-based proteomics for both experiments to identify proteins that were associated with PTGFRN. Our data show that PTGFRN knockdown increased pathways related to innate immune responses and decreased pathways associated with the synthesis of metabolic precursors and protein processing, among others. Additionally, the coimmunoprecipitation experiments indicated that PTGFRN is associated with proteins involved in processing and metabolism, as well as VEGF signaling molecules. These results highlight the role of PTGFRN as a protein processing regulator, which may be influencing cancer progression.

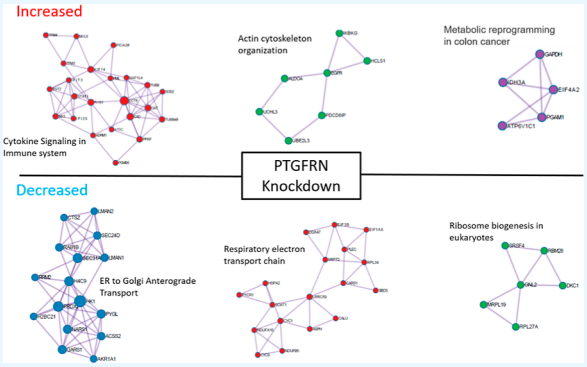

INTRODUCTION

Prostaglandin F2 receptor negative regulator, or PTGFRN, is a transmembrane protein whose primary binding partners are CD9 and CD81, two proteins that are members of a family of proteins called tetraspanins. This is a family of structurally homologous proteins involved in a multitude of cellular processes, such as adhesion, migration, cell differentiation, protein trafficking, and cancer malignancy, among others.[1] Tetraspanins are capable of binding not only to other tetraspanins but also to proteins outside of the tetraspanin family, such as PTGFRN, integrins, immunoglobulin superfamily members, and matrix metalloproteinases.[2] This complex network of protein associations makes up what is referred as the tetraspanin web.[3] PTGFRN has been found to bind primarily to tetraspanins CD9, CD81, and CD151 (only when complexed with CD9), although it has been found to be associated with a host of other nontetraspanin proteins, such as Integrin β1, LMBR1L, and CD160.[4−6] While its exact role(s) in cancer progression has yet to be fully elucidated, previous research has pointed to its possible involvement in VEGF-mediated angiogenesis, its increased expression in metastatic cells compared to their nonmetastatic counterparts, and the positive correlation between its expression level and poorer survival outcomes in glioblastoma patients.[7−9] Our laboratory has previously published evidence of PTGFRN being expressed and internalized in several cancer cells, and reported that treatment with an anti-PTFRN antibody drug conjugate led to inhibition of in vitro proliferation and in vivo tumor formation.[10] In this study, we performed a global proteomics analysis on human epidermoid carcinoma cells (A431) whose PTGFRN expression was decreased by stable shRNA knockdown in order to better understand the cellular processes affected by PTGFRN knockdown. We also performed coimmunoprecipitation experiments using a monoclonal antibody specific to PTGFRN, followed by mass spectrometric analysis in order to assess what proteins are associated with PTGFRN, and the pathways represented by these binding partners.

MATERIALS AND METHODS

Cell Lines. A431 cells were obtained from the American Type Culture Collection (ATCC, Manassas, VA). A431 (CRL-1555) was cultured in Dulbecco's Modified Eagle Medium/Ham's F12 medium (DMEM/F12 1:1 mixture) supplemented with 50 μg/mL gentamycin and 5% FBS and maintained in a 5% CO_2 incubator at 37 °C.

Received: January 2, 2024
Revised: February 7, 2024
Accepted: February 14, 2024
Published: March 15, 2024

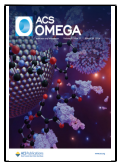

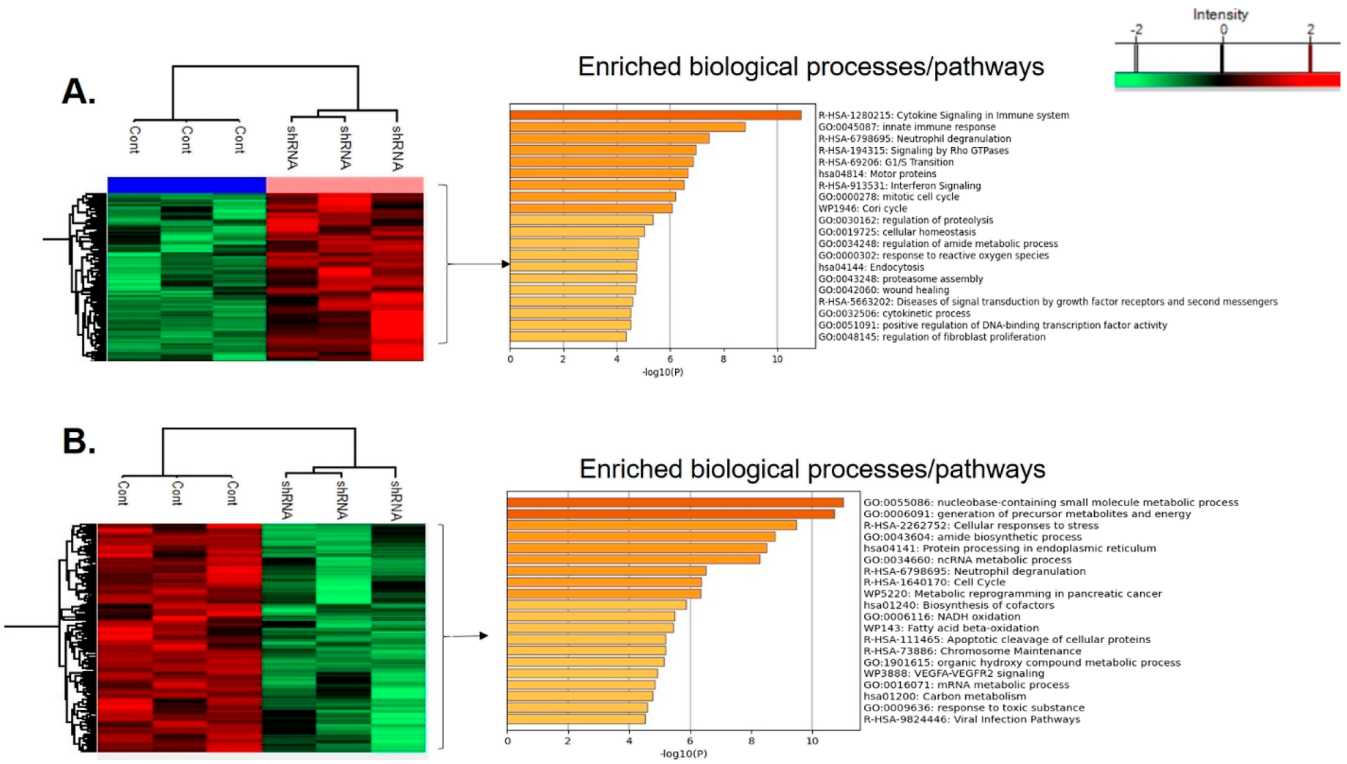

Figure 1. Mass spectrometric proteome analysis after PTGFRN knockdown. Heatmap displaying (A) the top 20 cellular processes upregulated after PTGFRN knockdown based on upregulated protein expression and (B) the top 20 cellular processes downregulated after PTGFRN knockdown based on downregulated protein expression. Statistical significance was determined by Student *t*-test analysis. All results shown meet the threshold of $p < 0.05$.

Silencing/Overexpression of PTGFRN and Clone Screening. A431 cells were stably transfected with two different human PTGFRN shRNAs (Fenics Bio, HSH321177-100), in order to silence PTGFRN expression (shRNA #1 sequence: TAGCCTTAAGAATGAATATGAA; shRNA #2 sequence: GTGGTATGTTTTGCTTTCCTAA), as well as one scrambled shRNA as a control. Transfections were carried out with the Lipofectamine 3000 reagent (Thermo Fisher, L3000015), according to the manufacturer's instructions. After transfection, the pooled cells were sorted and dispensed as single cells into a 96-well plate by the Hana Single-Cell Dispenser (Namocell, #NI004). These single-cell clones were then expanded and screened via flow cytometry and immunoblotting for the lowest PTGFRN-expressing clone. All immunoprecipitated proteins were subjected to a mass spectrometry analysis.

Coimmunoprecipitation. Experiments were carried out in triplicate. A431 was lysed in 1% Brij-O10 lysis buffer containing protease inhibitor cocktail, and this lysate was precleared with 100 μL of packed protein G agarose beads (Protein Mods) overnight at 4 °C. The next day, aliquots of lysates (250 μg each) were incubated with 10 μg of either control human IgG or anti-PTGFRN human monoclonal antibody 8C7 (generated in-house) overnight at 4 °C. The next day, protein G agarose beads were added to the lysates and mixed for 2 h. After 5 washes with 1% Brij lysis buffer, 2X SDS+DTT sample buffer was added to the beads. All immunoprecipitated proteins were subjected to mass spectrometry analysis.

Mass Spectrometry-Based Proteomics Analysis. Cell lysis and protein digestion were performed as previously described.[11] Briefly, samples were lysed in a lysis buffer containing 5% sodium dodecyl sulfate (Sigma, L4509) and 50 mM triethylammonium bicarbonate (1 M, pH 8.0) (Sigma, 7408). Proteins were extracted and digested using S-trap micro columns (ProtiFi, NY). The eluted peptides from the S-trap column were dried, and the peptide concentration was determined using a BCA assay kit (Thermo Fisher Scientific, 23275), after reconstitution in 0.1% formic acid. All tryptic peptides were separated on a nanoACQUITY Ultra-Performance Liquid Chromatography analytical column (BEH130 C18, 1.7 μm, 75 μm × 200 mm; Waters Corporation, Milford, MA, USA) over a 185 min linear acetonitrile gradient (3−40%) with 0.1% formic acid on a nanoACQUITY Ultra-Performance Liquid Chromatography system (Waters Corporation, Milford, MA USA) and analyzed on a coupled Orbitrap Fusion Lumos Tribrid mass spectrometer (Thermo Scientific, San Jose, CA USA). Full scans were acquired at a resolution of 240,000m/z, and precursors were selected for fragmentation by high-energy collisional dissociation of 35% for a maximum 3 s cycle. The MS/MS raw files were processed with Proteome Discoverer, version 2.5.0.400 (Thermo Fisher Scientific) using a Sequest HT search engine against a UniProt human reference proteome (release 2022.04, 20292 entries). Searches were configured with static modifications for carbamidomethyl on cysteines (+57.021 Da), dynamic modifications for oxidation of methionine residues (+15.995 Da), precursor mass tolerance of 20 ppm, and fragment mass tolerance of 0.5 Da. Trypsin was used as a digestion enzyme with a maximum of two missed cleavages. The minimum and maximum peptide lengths were set as 6 and 144, respectively. Label-free quantification was performed using Minora feature detector, a tool embedded in the PD bioinformatics platform.[12] For analysis of results, protein identification was filtered to a 1%

https://doi.org/10.1021/acsomega.4c00042
ACS Omega 2024, 9, 14381−14387

false discovery rate (FDR) in peptide spectra match (PSM), peptide, and protein levels. The FDR was calculated using the Percolator algorithm embedded in PD. Next, the exported protein abundance values were analyzed and visualized using Perseus software (version 1.6.14.0).[13] To ensure high confidence in statistical analysis, data were further filtered to include only proteins identified without any missing values in all of the biological samples. The quantitative protein data were $\log_2$ transformed and further normalized using median centering. The two-tailed Student's *t*-test was applied for comparisons between two conditions ($p < 0.05$) to determine if each treatment group was significantly different from the control group. Enrichment of functions and signaling pathways of the differentially expressed proteins (DEPs) identified from different conditions was performed using Metascape (http://metascape.org) as described previously.[11,14] Once the DEPs were identified, we subsequently used bioinformatics pathway analysis to further infer perturbed pathways. Ingenuity Pathway Analysis (IPA) was also used to predict canonical pathways and upstream regulators.[15,16]

RESULTS

Effect of PTGFRN Expression on the Proteomic Profile of A431 Cells. The aim of our current study was to investigate the effect of PTGFRN knockdown on the proteome of A431 cells. To this end, we performed mass spectrometric analysis on A431 cells where PTGFRN expression had been inhibited by shRNA transfection (A431 shRNA) and on control A431 cells transfected with a scrambled shRNA sequence, cultivated under 2D culture conditions. The proteomic analysis resulted in the identification of 5680 protein groups (Table S1) at 1% FDR after filtering the processed data as described in the Materials and Methods section. Among these protein groups, 3455 were quantified without missing values in any of the 12 samples. We next assessed any protein whose expression was significantly increased or decreased in response to PTGFRN knockdown. Using the list of modulated proteins, we performed pathway analysis using Metascape or IPA in order to determine what cellular functions and pathways were most affected by the decrease in PTGFRN expression.

After PTGFRN knockdown, the most downregulated biological processes or pathways were involved in the synthesis of various metabolites, metabolic precursors, and energy, including those involved in the respiratory electron transport chain. In addition to this, other significantly inhibited pathways include Endoplasmic Reticulum to Golgi anterograde transport, ribosome biogenesis, exosome function, NADH oxidation, and VEGFA-VEGFR2 signaling. PTGFRN knockdown also resulted in increases in other pathways, with many of them involved in immune system signaling, such as cytokine signaling, interferon signaling, and neutrophil degranulation. The heatmap in Figure 1A outlines the top 20 cellular processes that were increased after PTGFRN knockdown by shRNA transfection, while Figure 1B shows the top 20 cellular processes that were found to be decreased after PTGFRN knockdown. Table 1 contains the top 10 proteins found to be upregulated after PTGFRN knockdown, while Table 2 outlines the top 10 pathways represented by those proteins upregulated after PTGFRN knockdown. Table 3 presents the top 10 proteins whose expression was downregulated after PTGFRN knockdown, followed by Table 4, which describes the pathways most impacted by the downregulated proteins. The complete list of all impacted pathways and protein members after PTGFRN knockdown can be found in Supplementary Tables (Tables S2−S5).

Table 1. Top 10 Most Upregulated Proteins after PTGFRN Knockdown[a]

accession number	gene name	protein description	fold-increase
Q92817	EVPL	component of desmosome and epidermal cornified envelope	9.3
P06702	S100A9	calcium-binding protein	3.4
O95786	RIGI	RNA helicase-DEAD box protein	3.2
P01583	IL1A	interleukin 1 alpha; cytokine	3.1
O95999	BCL10	immune signaling adaptor	3.0
P01833	PIGR	IgA/IgM transport receptor	2.9
P29966	MARCKS	substrate for protein kinase C	2.7
P80188	LCN2	hydrophobic molecule transporter	2.4
Q9Y316	MEMO1	regulator of cell motility	2.4
P14317	HCLS1	actin-binding protein	2.4

[a]The full list of upregulated proteins is provided in the Supporting Information as Table S2.

Table 2. Top 10 Most Upregulated Cellular Pathways after PTGFRN Knockdown[a]

pathway	adjusted *p*-value	*Z*-score
cytokine signaling in immune system	2.87×10^{-7}	2.44
innate immune response	1.78×10^{-5}	N/A
neutrophil degranulation	2.02×10^{-4}	N/A
signaling by Rho GTPases	4.98×10^{-4}	N/A
G1/S transition	4.98×10^{-4}	N/A
motor proteins	6.35×10^{-4}	N/A
nterferon signaling	6.44×10^{-4}	2.0
mitotic cell cycle	8.65×10^{-4}	0.447
cori cycle	1.06×10^{-3}	N/A
regulation of proteolysis	3.15×10^{-3}	N/A

[a]The full list of upregulated pathways is provided in the Supporting Information as Table S3. Full IPA analysis can be found in Table S8.

Table 3. Top 10 Most Downregulated Proteins after PTGFRN Knockdown[a]

accession number	gene name	protein description	percent decrease (%)
Q8IVL5	P3H2	post-translational 3-hydroxylation enzyme	90
Q14155	ARHGEF7	Rho protein activator	81
Q8NHV4	NEDD1	centrosome interactor with γ-tubulin	79
P54652	HSPA2	heat-shock protein, protein folding chaperone	73
P13646	KRT13	keratin 13	72
Q8N1T3	MYO1H	microfilament binding and organization	65
Q9UK22	FBXO2	ubiquitin protein transferase enzyme	64
P13647	KRT5	keratin 5	59
Q16658	FSCN1	F-actin organization	58
O95260	ATE1	arginyl-tRNA-protein transferase	57

[a]The full list of downregulated proteins is provided in the Supporting Information as Table S4.

PTGFRN Interactome Analysis. In addition to looking at the effect of PTGFRN expression modulation, we also applied mass spectrometric analysis to examine proteins that were

https://doi.org/10.1021/acsomega.4c00042
ACS Omega 2024, 9, 14381−14387

Table 4. Top 10 Most Downregulated Cellular Pathways after PTGFRN Knockdown[a]

pathway	adjusted p-value	Z-score
nucleobase-containing small-molecule metabolic process	2.15×10^{-7}	−1.0
generation of precursor metabolites and energy	2.18×10^{-7}	N/A
cellular responses to stress	1.87×10^{-6}	−0.445
amide biosynthetic process	7.71×10^{-6}	−2.0
protein processing in endoplasmic reticulum	9.02×10^{-6}	N/A
ncRNA metabolic process	1.18×10^{-5}	−2.45
neutrophil degranulation	2.82×10^{-4}	N/A
cell cycle	3.19×10^{-4}	N/A
metabolic reprogramming in pancreatic cancer	3.19×10^{-4}	−1.0
biosynthesis of cofactors	8.11×10^{-4}	−1.0

[a]The full list of downregulated pathways is provided in the Supporting Information as Table S5. Full IPA analysis can be found in Table S8.

Table 5. Top 10 Most Abundant Proteins in PTGFRN Coimmunoprecipitation with 8C7[a]

accession number	gene name	protein description
P08579	SNRPB2	ribonuclear protein
P50851	LRBA	cellular component recycler in autophagy
O60294	LCMT2	leucine carboxyl methyltransferase 2
Q8IWA5	SLC44A2	choline transporter
Q9ULC3	RAB23	vesicle trafficking protein
Q02878	RPL6	ribosomal protein
Q13685	AAMP	angio-associated migratory cell protein
Q8N573	OXR1	oxidation resistance protein
Q9Y5 V0	ZNF706	zinc-finger protein
Q9HCU5	PREB	transcription factor that regulates prolactin (PRL) gene expression

[a]The full list of coimmunoprecipitated proteins is provided in the Supporting Information as Table S6.

Table 6. Top 10 Cellular Pathways Represented in PTGFRN Coimmunoprecipitation with 8C7[a]

pathway	adjusted *p*-value	Z-score
metabolism of RNA	6.20×10^{-29}	0.816
VEGFA-VEGFR2 signaling	2.60×10^{-11}	1.0
ribonucleoprotein complex biogenesis	1.66×10^{-8}	0.816
regulation of translation	8.59×10^{-8}	N/A
CLEC7A (Dectin-1) signaling	4.49×10^{-7}	N/A
actin filament organization	2.76×10^{-6}	1.155
mRNA metabolic process	3.12×10^{-6}	N/A
protein processing in the endoplasmic reticulum	8.79×10^{-6}	N/A
RHO GTPase cycle	1.74×10^{-5}	1.155
fragile X syndrome	2.52×10^{-5}	N/A

[a]The full list of pathways is provided in the Supporting Information as Table S7. Full IPA analysis can be found in Table S9.

associated with PTGFRN by coimmunoprecipitation with an anti-PTGFRN antibody compared to coimmunoprecipitation with control IgG. From this list of proteins found to coimmunoprecipitate with PTGFRN, pathway analysis was also performed, indicating which processes had protein members that were either directly bound to or associated with PTGFRN.

The cellular process that had by far the most members found to be associated with PTGFRN was the metabolism of RNA. The pathways VEGFA-VEGFR2 signaling, regulation of translation, and ribonucleoprotein complex biogenesis also had many protein constituents pulled down along with PTGFRN. Figure 2 displays the heatmap outlining the top 20 processes whose protein members were found to coimmunoprecipitate with PTGFRN, indicating protein interactions. Table 5 displays the top 10 proteins that were the most abundantly present besides PTGFRN after co-IP with 8C7, while Table 6 contains the top 10 pathways associated with these coimmunoprecipitated proteins. The full list of all proteins coimmunoprecipitated with PTGFRN and the potentially impacted pathways can be found in the Supporting Information (Tables S6 and S7).

DISCUSSION

The mass spectrometric analysis performed here provided new data about the effect of PTGFRN expression on the proteomic profile and proteins associated with PTGFRN. First, the cellular processes whose protein members were decreased in expression after PTGFRN knockdown (Table 3) appear to

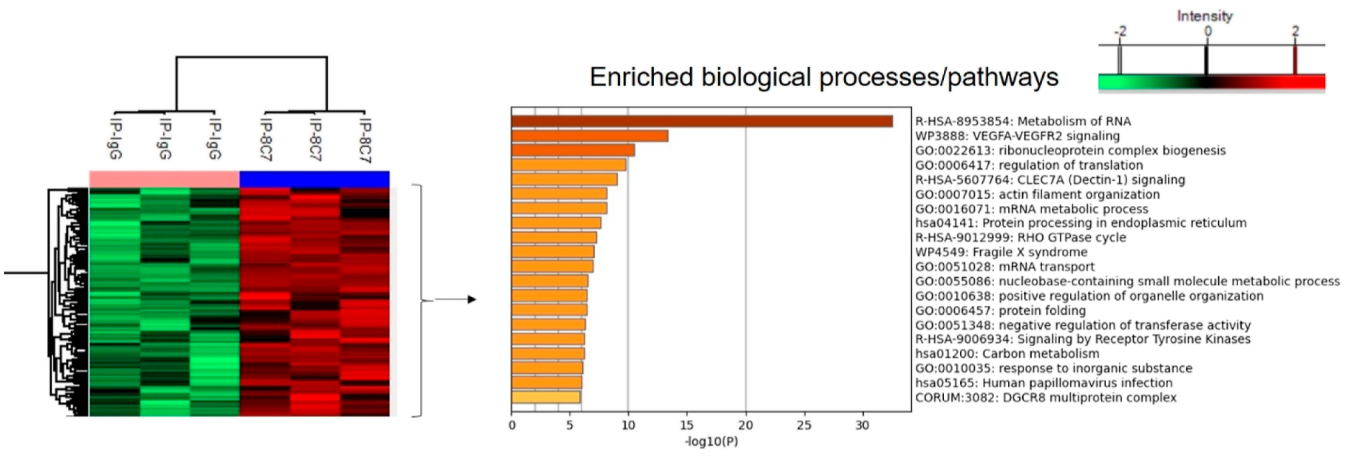

Figure 2. Mass spectrometric analysis of PTGFRN co-IP products. Heatmap displaying the top 20 cellular processes whose protein members were found to be enriched in the 8C7 co-IP samples compared to an IgG control antibody. Statistical significance was determined by the Student *t*-test analysis. All results shown meet the threshold of $p < 0.05$.

https://doi.org/10.1021/acsomega.4c00042
ACS Omega 2024, 9, 14381−14387

validate findings already reported for PTGFRN, where PTGFRN knockdown was found to inhibit VEGF-induced angiogenesis, and overexpression was found to be correlated with a metastatic-like profile.[8,9,17] The inability to biosynthesize metabolic precursors, transport proteins for appropriate post-translational modification, or even produce normal levels of ATP from NADH oxidation and the electron transport chain would certainly likely result in diminished ability for cells to proliferate and would severely limit how many cells could grow into colonies from a single cell if the said cell has lower proliferative capability. Second, while cellular migration was not a pathway listed in the database used to examine the proteomics data, there are indeed proteins found to be involved in the migration and invasion whose expression was decreased after PTGFRN knockdown (Table S4 in Supplementary Information). The proteins NUDT1, DKC1, RBBP7, and RSF-1 (all contained within the chromosome maintenance pathway), as well as LRRC59 (VEGFA-VEGFR2 signaling pathway), shown here to be decreased in expression after PTGFRN knockdown, have all been found to be involved in and influence the migration capability of cancer cells.[18−22] Elevated proliferation, migration, and clonogenic potentials are all hallmarks of metastatic cancer cells.[23] Our laboratory has also evaluated the effect of PTGFRN knockdown in A431 cells in functional cell-based assays. The results of these investigations show that PTGFRN expression is directly correlated to the ability of A431 cells to proliferate, migrate, grow in colonies, and form 3D spheroids (manuscript under review for publication). The ability of PTGFRN knockdown to significantly inhibit proliferation in A431 cells is especially of note, as these cells express high levels of the cell surface receptor EGFR, which has been found to significantly increase the proliferation of nearly all cell types.[24,25]

When analyzing the proteins that are directly bound/complexed with PTGFRN and coimmunoprecipitate alongside PTGFRN with an anti-PTGFRN antibody, it should first be noted that the two most well-studied binding partners of PTGFRN, the tetraspanins CD9 and CD81, were both found to have immunoprecipitated with PTGFRN in our experiments detailed here (Table S1). This can be regarded as an internal control, contributing to the reinforcement of our confidence in the validity of the remaining presented data. The pathway whose members showed the most interaction with PTGFRN was metabolism of RNA. In fact, of the top 20 pathways whose proteins are found to be bound to PTGFRN, 9 of them are involved directly or indirectly in RNA processing or translation (Table S6). Proteins involved in the formation of the ribosome subunits (RPL3 and RPS8), , removal of introns from pre-mRNA (SNRPB2), and translation initiation factors (EIF2a) were among the most abundantly coimmunoprecipitated along with PTGFRN. This is quite interesting, as these proteins are typically found in the cytoplasm, located nearby the endoplasmic reticulum,[26] whereas PTGFRN is most commonly found in the plasma membrane. This would suggest that PTGFRN serves as a membrane anchor, working as a part of a large scaffold to stabilize the ribosome, various polymerases, and/or translation factors so that they can properly process RNA. PTGFRN could also be functioning solely as a trafficking protein to ensure that these components reach their required subcellular locations from the Golgi apparatus while not actually contributing to their overall function. Alternatively, these results could also point to an intracellular form of PTGFRN whose functions differ from those associated with its plasma membrane form. It is unclear at this time if these differing functions could be due to distinct isoforms through alternative splicing or different glycosylation patterns or if the subcellular location of PTGFRN influences its overall function. It is known that PTGFRN may have 3 putative splice sites, which could very well result in different isoforms with differing functions.[27]

The next most abundantly represented pathway whose protein members were found to co-IP with PTGFRN was that of VEGFA−VEGFR2 signaling. Interestingly, the same pathway was also found to be significantly decreased following PTGFRN knockdown. Notably, the only protein whose expression was found to be both downregulated after PTGFRN knockdown as well as coimmunoprecipitated with PTGFRN in our co-IP, was LMAN1, a protein found to regulate protein folding, transport to the Golgi from the endoplasmic reticulum, and other organelle organization.[28] This lends further support to the hypothesis that PTGFRN seems to be highly involved in RNA processing and translation and the trafficking of the newly translated protein to the Golgi and further cellular locations. These results seemingly confirm those published by Colin et al., where it was demonstrated that transfection of a truncated form of PTGFRN into cells resulted in diminished angiogenesis and thus tumor formation.[7]

Taken all together, the analysis performed here provides proteomic information to support previously published observations, linking PTGFRN to VEGF-induced angiogenesis and also further establishing a relationship between PTGFRN expression and cancer metastasis. Additionally, the discovery that PTGFRN seems to be overwhelmingly associated with proteins involved in mRNA and protein translation/trafficking contributes other mechanisms by which PTGFRN affects cell proliferation and migration, contributing to cancer metastasis.

CONCLUSIONS

In summary, mass spectrometric analysis sheds new light on the effect of PTGFRN expression on the proteome of A431 cells. Previously published findings were also confirmed, such as PTGFRN's role in VEGF signaling. Interactome analysis also provided added information regarding PTGFRN binding partners, showing PTGFRN association with proteins involved in mRNA/protein translation and processing. This information provides some pathways with which PTGFRN expression may affect cancer cell phenotype and how it may correlate with a metastatic-like profile, as previously reported.

ASSOCIATED CONTENT

Supporting Information

The Supporting Information is available free of charge at https://pubs.acs.org/doi/10.1021/acsomega.4c00042.

All proteins identified from label-free proteomics data, upregulated proteins after PTGFRN knockdown identified by t-test, upregulated pathways after PTGFRN knockdown identified by t-test, downregulated proteins after PTGFRN knockdown identified by t-test, downregulated pathways after PTGFRN knockdown identified by t-test, upregulated proteins in IP-8C7 vs. IP-IgG identified by t-test, upregulated pathways in IP-8C7 vs. IP-IgG identified by t-test, IPA Pathway Analysis after PTGFRN knockdown, and IPA pathway analysis of anti-PTGFRN 8C7 coimmunoprecipitated proteins (XLSX)

https://doi.org/10.1021/acsomega.4c00042
ACS Omega 2024, 9, 14381−14387

AUTHOR INFORMATION

Corresponding Author

Ginette Serrero − *Target Discovery Division, A&G Pharmaceutical, Inc., Columbia, Maryland 21045, United States of America*; Phone: (410) 884-4100; Email: gserrero@agpharma.com

Authors

Jorge Marquez − *Department of Pharmaceutical Sciences, University of Maryland School of Pharmacy, Baltimore, Maryland 21201, United States of America; Target Discovery Division, A&G Pharmaceutical, Inc., Columbia, Maryland 21045, United States of America;* orcid.org/0009-0000-5795-0638

Mehari M. Weldemariam − *Department of Pharmaceutical Sciences, University of Maryland School of Pharmacy, Baltimore, Maryland 21201, United States of America*

Jianping Dong − *Target Discovery Division, A&G Pharmaceutical, Inc., Columbia, Maryland 21045, United States of America*

Jun Hayashi − *Precision Antibody Service, Suite X Columbia, Maryland 21045, United States*

Maureen A. Kane − *Department of Pharmaceutical Sciences, University of Maryland School of Pharmacy, Baltimore, Maryland 21201, United States of America;* orcid.org/0000-0002-5525-9170

Complete contact information is available at: https://pubs.acs.org/10.1021/acsomega.4c00042

Author Contributions

The manuscript was written through contributions of all authors. All authors have given approval to the final version of the manuscript.

Funding

This work was funded in part by grants from the National Cancer Institute (R44CA224718 and R44CA162629) to Ginette Serrero. Additional support was provided by the University of Maryland School of Pharmacy Mass Spectrometry Center (SOP1841-IQB2014).

Notes

The authors declare no competing financial interest.

ABBREVIATIONS

DEP, Differentially expressed proteins; FDR, False discovery rate; IP, Immunoprecipitation; PSM, Peptide spectra match; PTGFRN, Prostaglandin F2 receptor negative regulator

ADDITIONAL NOTE

PRIDE The mass spectrometry proteomics data have been deposited to the ProteomeXchange Consortium via the partner repository with the data set identifier PXD048092.

REFERENCES

(1) Jiang, X.; Zhang, J.; Huang, Y. Tetraspanins in Cell Migration. *Cell Adhes. Migr.* **2015**, *9* (5), 406−415.

(2) Hemler, M. E. Targeting of tetraspanin proteins—potential benefits and strategies. *Nat. Rev. Drug Discov.* **2008**, *7* (9), 747−758.

(3) van Deventer, S. J.; Dunlock, V.-M. E.; van Spriel, A. B. Molecular interactions shaping the tetraspanin web. *Biochem. Soc. Trans.* **2017**, *45* (3), 741−750.

(4) Charrin, S.; Le Naour, F.; Oualid, M.; Billard, M.; Faure, G.; Hanash, S. M.; Boucheix, C.; Rubinstein, E. The Major CD9 and CD81 Molecular Partner: IDENTIFICATION AND CHARACTERIZATION OF THE COMPLEXES *. *J. Biol. Chem.* **2001**, *276* (17), 14329−14337.

(5) Choi, J. H.; Zhong, X.; McAlpine, W.; Liao, T.-C.; Zhang, D.; Fang, B.; Russell, J.; Ludwig, S.; Nair-Gill, E.; Zhang, Z.; et al. LMBR1L regulates lymphopoiesis through Wnt/β-catenin signaling. *Science (80-)* **2019**, *364* (6440), No. eaau0812.

(6) Huttlin, E. L.; Bruckner, R. J.; Navarrete-Perea, J.; Cannon, J. R.; Baltier, K.; Gebreab, F.; Gygi, M. P.; Thornock, A.; Zarraga, G.; Tam, S.; et al. Dual proteome-scale networks reveal cell-specific remodeling of the human interactome. *Cell* **2021**, *184* (11), 3022.e28−3040.e28.

(7) Colin, S.; Guilmain, W.; Creoff, E.; Schneider, C.; Steverlynck, C.; Bongaerts, M.; Legrand, E.; Vannier, J. P.; Muraine, M.; Vasse, M.; et al. A truncated form of CD9-partner 1 (CD9P-1), GS-168AT2, potently inhibits in vivo tumour-induced angiogenesis and tumour growth. *Br. J. Cancer* **2011**, *105* (7), 1002−1011.

(8) Karhemo, P. R.; Ravela, S.; Laakso, M.; Ritamo, I.; Tatti, O.; Mäkinen, S.; Goodison, S.; Stenman, U. H.; Hölttä, E.; Hautaniemi, S.; et al. An optimized isolation of biotinylated cell surface proteins reveals novel players in cancer metastasis. *J. Proteomics* **2012**, *77*, 87−100.

(9) Aguila, B.; Morris, A. B.; Spina, R.; Bar, E.; Schraner, J.; Vinkler, R.; Sohn, J. W.; Welford, S. M. The Ig superfamily protein PTGFRN coordinates survival signaling in Glioblastoma multiforme. *Cancer Lett.* **2019**, *462*, 33−42.

(10) Marquez, J.; Dong, J.; Dong, C.; Tian, C.; Serrero, G. Identification of Prostaglandin F2 Receptor Negative Regulator (PTGFRN) as an internalizable target in cancer cells for antibody-drug conjugate development. *PLoS One* **2021**, *16*, No. e0246197.

(11) Weldemariam, M. M.; Sudhir, P.-R.; Woo, J.; Zhang, Q. Effects of multiple stressors on pancreatic human islets proteome reveal new insights into the pathways involved. *Proteomics* **2023**, *23* (19), 2300022.

(12) Palomba, A.; Abbondio, M.; Fiorito, G.; Uzzau, S.; Pagnozzi, D.; Tanca, A. Comparative Evaluation of MaxQuant and Proteome Discoverer MS1-Based Protein Quantification Tools. *J. Proteome Res.* **2021**, *20* (7), 3497−3507. Available from: https://pubmed.ncbi.nlm.nih.gov/34038140

(13) Tyanova, S.; Temu, T.; Sinitcyn, P.; Carlson, A.; Hein, M. Y.; Geiger, T.; Mann, M.; Cox, J. The Perseus computational platform for comprehensive analysis of (prote)omics data. *Nat. Methods* **2016**, *13* (9), 731−740.

(14) Zhou, Y.; Zhou, B.; Pache, L.; Chang, M.; Khodabakhshi, A. H.; Tanaseichuk, O.; Benner, C.; Chanda, S. K. Metascape provides a biologist-oriented resource for the analysis of systems-level datasets. *Nat. Commun.* **2019**, *10* (1), 1523.

(15) Krämer, A.; Green, J.; Pollard Jr, J.; Tugendreich, S. Causal analysis approaches in Ingenuity Pathway Analysis. *Bioinformatics* **2014**, *30* (4), 523−530.

(16) Huang, W.; Yu, J.; Liu, T.; Tudor, G.; Defnet, A. E.; Zalesak, S.; Kumar, P.; Booth, C.; Farese, A. M.; MacVittie, T. J.; et al. Proteomic Evaluation of the Natural History of the Acute Radiation Syndrome of the Gastrointestinal Tract in a Non-human Primate Model of Partial-body Irradiation with Minimal Bone Marrow Sparing Includes Dysregulation of the Retinoid Pathway. *Health Phys.* **2020**, *119* (5), 604−620. Available from: https://journals.lww.com/health-physics/fulltext/2020/11000/proteomic_evaluation_of_the_natural_history_of_the.6.aspx

(17) Guilmain, W.; Colin, S.; Legrand, E.; Vannier, J. P.; Steverlynck, C.; Bongaerts, M.; Vasse, M.; Al-Mahmood, S. CD9P-1 expression correlates with the metastatic status of lung cancer, and a truncated form of CD9P-1, GS-168AT2, inhibits in vivo tumour growth. *Br. J. Cancer* **2011**, *104* (3), 496−504.

(18) Ou, Q.; Ma, N.; Yu, Z.; Wang, R.; Hou, Y.; Wang, Z.; Chen, F.; Li, W.; Bi, J.; Ma, J.; et al. Nudix hydrolase 1 is a prognostic biomarker in hepatocellular carcinoma. *Aging (Albany NY)* **2020**, *12* (8), 7363−7379. Available from: https://pubmed.ncbi.nlm.nih.gov/32341205

(19) Miao, F.; Chu, K.; Chen, H.; Zhang, M.; Shi, P.; Bai, J.; You, Y. p. Increased DKC1 expression in glioma and its significance in tumor

cell proliferation, migration and invasion. *Invest New Drugs* **2019**, *37* (6), 1177−1186.
(20) Yu, N.; Zhang, P.; Wang, L.; He, X.; Yang, S.; Lu, H. RBBP7 is a prognostic biomarker in patients with esophageal squamous cell carcinoma. *Oncol Lett.* **2018**, *16* (6), 7204−7211. Available from: https://pubmed.ncbi.nlm.nih.gov/30546458
(21) Zhang, X.; Fu, L.; Xue, D.; Zhang, X.; Hao, F.; Xie, L.; He, J.; Gai, J.; Liu, Y.; Xu, H.; et al. Overexpression of Rsf-1 correlates with poor survival and promotes invasion in non-small cell lung cancer. *Virchows Arch.* **2017**, *470* (5), 553−560.
(22) Li, D.; Xing, Y.; Tian, T.; Guo, Y.; Qian, J. Overexpression of LRRC59 Is Associated with Poor Prognosis and Promotes Cell Proliferation and Invasion in Lung Adenocarcinoma. *OncoTargets Ther.* **2020**, *13*, 6453−6463. Available from: https://pubmed.ncbi.nlm.nih.gov/32753886
(23) Fares, J.; Fares, M. Y.; Khachfe, H. H.; Salhab, H. A.; Fares, Y. Molecular principles of metastasis: a hallmark of cancer revisited. *Signal Transduction Targeted Ther.* **2020**, *5* (1), 28.
(24) Zhou, P.; Hu, J.; Wang, X.; Wang, J.; Zhang, Y.; Wang, C. Epidermal growth factor receptor expression affects proliferation and apoptosis in non-small cell lung cancer cells via the extracellular signal-regulated kinase/microRNA 200a signaling pathway. *Oncol Lett.* **2018**, *15* (4), 5201−5207.
(25) Zhang, F.; Wang, S.; Yin, L.; Yang, Y.; Guan, Y.; Wang, W.; Xu, H.; Tao, N. Quantification of Epidermal Growth Factor Receptor Expression Level and Binding Kinetics on Cell Surfaces by Surface Plasmon Resonance Imaging. *Anal. Chem.* **2015**, *87* (19), 9960−9965. Oct 6, Available from
(26) Reid, D. W.; Nicchitta, C. V. Primary role for endoplasmic reticulum-bound ribosomes in cellular translation identified by ribosome profiling. *J. Biol. Chem.* **2012**, *287* (8), 5518−5527. Available from: https://pubmed.ncbi.nlm.nih.gov/22199352
(27) Cunningham, F.; Allen, J. E.; Allen, J.; Alvarez-Jarreta, J.; Amode, M. R.; Armean, I. M.; Austine-Orimoloye, O.; Azov, A.; Barnes, I.; Bennett, R.; et al. Ensembl 2022. *Nucleic Acids Res.* **2022**, *50* (D1), D988−D995.
(28) Cunningham, M. A.; Pipe, S. W.; Zhang, B.; Hauri, H.-P.; Ginsburg, D.; Kaufman, R. J. LMAN1 is a molecular chaperone for the secretion of coagulation factor VIII. *J. Thromb. Haemost.* **2003**, *1* (11), 2360−2367. Available from: https://www.sciencedirect.com/science/article/pii/S153878362215484X

https://doi.org/10.1021/acsomega.4c00042
ACS Omega 2024, 9, 14381−14387